

SCALE UNIFICATION – A UNIVERSAL SCALING LAW FOR ORGANIZED MATTER

Nassim Hamein,[†] Michael Hyson,[‡] E. A. Rauscher[§]

Abstract. From observational data and our theoretical analysis, we demonstrate that a scaling law can be written for all organized matter utilizing the Schwarzschild condition, describing cosmological to sub-atomic structures. Of interest are solutions involving torque and Coriolis effects in the field equations. Significant observations have led to theoretical and experimental advancement describing systems undergoing gravitational collapse, including vacuum interactions. The universality of this scaling law suggests an underlying polarizable structured vacuum of mini white holes/black holes. We briefly discuss the manner in which this structured vacuum can be described in terms of resolution of scale analogous to a fractal-like scaling as a means of renormalization at the Planck distance. Finally, we describe a new horizon we term the “spin horizon” which is defined as a result of a spacetime torque producing boundary conditions in a magnetohydrodynamic structure.

INTRODUCTION

In astrophysics, black holes have been ubiquitously confirmed from large scale super-giants such as quasars and galactic centers to smaller stellar size black hole systems. These new discoveries represent a long term progress to confirm the 1916 Schwarzschild solution to Einstein’s field equations. The observed black hole at the center of the Milky Way galaxy was first discovered by its gravitational influence on nearby stars. So far, black holes seem to have been found at the center of all galaxies that have been carefully examined [1]. Now, quasars and globular clusters, have been found to host large black holes and stellar black holes are well documented [1].

In this paper we develop a scaling law utilizing the Schwarzschild condition as well as discuss charge and rotation within a modified Kerr-Newman metric (the Hamein-Rauscher solution involving torque and Coriolis effects in the field equations [2]) for cosmological, galactic, stellar and micro physical black holes. It is important to note that all observed objects, from macro to micro, are predominantly x-ray emitters, which is typical of black hole horizons. At the horizon the gravitational force balances the electromagnetic radiation, a state previously thought to be only present at cosmogenesis, which implies a continuous creation model. This is based on the topology of “Schwarzschild’s zones” generating cells depicting a dynamic expanding and contracting universe first described by Wheeler and Lindquist [3]. Thermodynamic and acoustic processes occupy an important role in energy transfer between gravitational attraction, magnetohydrodynamic (MHD) and electrodynamic repulsion [4]. Solving the collective and coherent behavior of plasma MHD soliton structures, their thermo and acouston dynamics, results in a good description of the processes occurring externally, near and at the horizons of black holes [4]. A dual brane torus model of a U_4 group and the cuboctahedral cover group is utilized (see Appendix A). This approach leads to a polarized structured vacuum and an extended unified model. This model is a central feature of the Hameinian topological picture [4, 5, 6].

At the cosmological resolution, plasma dynamics surrounding the event horizon give us a good indication of the fundamental structure underlying the dynamical vacuum state polarization, its relationship to the event horizon [4, 7] and the topology of the spacetime manifold. Some recent observations by the Wide Field Planetary Camera 2 of the Hubble Space Telescope of Supernova SN1987A and Nebula MyCn18 (so-called Hourglass Nebula) and large galactic superstructures display certain qualities that relate to the plasma state field and its interaction with the vacuum structure producing double torus-like dynamics [8, 9, 10].

In this paper, we have developed a scaling law for the universal, galactic, stellar– solar and atomic scale frequencies vs. radius of the system, with the consideration of a fundamental response of these systems within the surrounding structured vacuum polarization, and we briefly discuss a new approach to renormalization. In this paper, we will touch on the details of the field topology and its interaction with the vacuum structure, and focus mostly on describing our scaling law where we compare our scaling rotation to the standard atomic model in which $1A \sim 10^{-8}$ cm. By way of comparison, we find the Big Bang cosmogenic parameters, $R \sim 10^{-33}$ cm and $\omega \sim 2 \times 10^{43}$ Hz and the current universe at $R \sim 10^{28}$ cm. We derive a scaling law and discuss possible explanations of the missing

[†] Director of Research, The Resonance Project Foundation, hamein@theresonanceproject.org

[‡] Research Director, Sirius Institute, michaelhyson@yahoo.com

[§] Tecnic Research Laboratory, 3500 S. Tomahawk Road, Bldg. 188, Apache Junction, AZ 85219

mass of the Universe in terms of vacuum state, polarizable and nonlinear structures which includes a new description of solar dynamics to generate the physics of a unified view [2, 4].

1. THE SCALING EQUATION FROM MACRO TO MICRO COSMOS IN TERMS OF FREQUENCY, ω VS. RADIUS, R

The primary constraint on the conditions relating the frequency of a system to its radius is through the Schwarzschild condition. Schwarzschild's 1916 solution is an extension solution to Einstein's gravitational field equations, which were published in 1915. The Schwarzschild solution is the most simple and elegant solution to the field equations for a spherical system. [11] This solution represents a space-time curvature structure produced by the presence of matter-energy. The field equations represent the universality of the gravitational force as represented by a spin 2 tensor gravitation, expressed as the curvature of four space or space-time. The Schwarzschild condition is given for the Schwarzschild radius, R_s and mass m_s , as

$$R_s \frac{2Gm_s}{c^2} \quad (1)$$

for the constant $\frac{2G}{c^2}$ where G is the gravitational constant and c is the velocity of light. This term is

$$\frac{2G}{c^2} = 1.48 \times 10^{-28} \text{ cm/gm}, \quad (2)$$

which we term $\Gamma = \frac{2G}{c^2}$, so that $R_s = \Gamma_{m_s}$.

J. A. Wheeler used the Schwarzschild solution as the solution for a *black hole*, a system in which gravity is so strong that light, once absorbed, cannot be reemitted. This led to the search for astrophysical black holes. He attempted to apply this description of the structure of space-time in order to explain the generation of the electromagnetic forces in terms of the micro "quantum" structure described by mini Planck black holes [12, 13, 14]. R.W. Lindquist and Wheeler also published work depicting a "dynamic lattice universe" based on the topology of Schwarzschild membrane zones arranged to generate cells [3] (See Fig. 1a).

This topological approach results in a dynamic expanding and contracting universe, where a test particle is found to rise and fall against the gravitational attraction. This author expresses a concentric black hole/white hole theorem by combining a Kerr-Newman charge and rotation metric of the Hamein-Rauscher solution [2] with the concept of an expanding and contracting Schwarzschild cell.

E.A. Rauscher [13], and more recently Hamein and Rauscher [2, 4, 14], developed a scaling law for physical variables as a function of the radius of the expanding universe. This cosmogenic model depends on the approximation that the universe obeys the Schwarzschild condition given by $R_s \sim 10^{-28} \text{ cm/gm} \times M_u$ yielding $R_u = R_s \sim 10^{28} \text{ cm}$ with the current universe radius at $R_u \sim 10^{28} \text{ cm}$ and a mass of $M_u \sim 10^{56} \text{ gm}$. The early Big Bang conditions, as conceived of, yields $R_s \sim 10^{-28} \text{ cm/gm} \times m_{pl}$ where m_{pl} is the mass of the initial Planck black hole of $m_{pl} \sim 10^{-5} \text{ gm}$ giving $R_s \sim \ell \sim 10^{-33} \text{ cm}$, the Planck length.

Hamein [5] and Rauscher [13] have developed a detailed scaling law for the characteristic frequency of a system and its radius [4]. This unique scaling law treats cosmological and micro systems in terms of black hole physics, under the Schwarzschild condition, for various systems, which are also ubiquitous x-ray emitters. This approach will be expanded to include the nature of a variety of black hole conditions. These conditions will not describe the detailed, more complex dynamics of each specific black hole system, but will, in general form, obey the first order Schwarzschild condition. Some of the more complex dynamics include x-ray emissions due to energy exchange of rotating and rotating-charged black holes [15, 16]. More appropriate descriptions of the origin of spin and its implications to the Field equations will yield new physics, such as the Hamein-Rauscher solution with torque and Coriolis forces [2]. Of particular interest is the description of local plasma and thermodynamic properties described by the Kerr and Kerr-Newman solutions for black holes, and the application of this understanding to micro-physics [4].

We can categorize the types of black hole solutions in the following manner. In general, a collapsing black hole system preserves its mass, electric charge and angular momentum or rotation. There are five general categories of black hole solutions. They are: (1) an uncharged, non-rotating black hole which is described by the Schwarzschild solution field equations, (2) a charged, non-rotating black hole which is described by the Reissner-Nordstrom solution, (3) an uncharged but rotating black hole which is described by the Kerr solution, (4) a rotating, charged black hole which is described by the Kerr-Newman solution and 5) the Hamein-Rauscher solution with the

inclusion of torque and Coriolis forces to define the origin of spin. [2] Returning to our Schwarzschild condition, we have calculated the conditions for micro to macro cosmological black holes [16]. Consider the usual Schwarzschild condition given above. Haremein, [5, 6] Rauscher [13, 17] and others have noted that at the universal scale for $R_u = 10^{28}$ cm and $M_u = 10^{56}$ gm and where

$$\Gamma = \frac{2G}{c^2} = 1.48 \times 10^{-28} \text{ cm/gm}, \quad (3)$$

we find a set of conditions for the entire universe as a black hole, i.e., the mass of our universe exceeds the mass of a system needed to overcome the escape velocity of light [12].

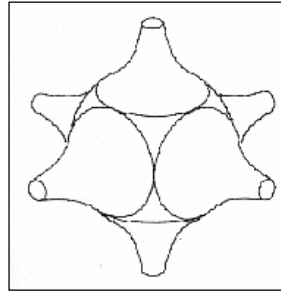


Figure 1(a)

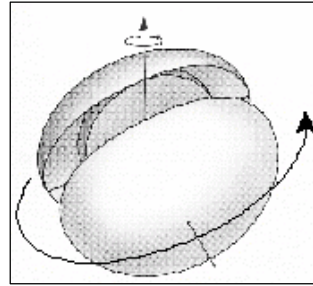


Figure 1(b)

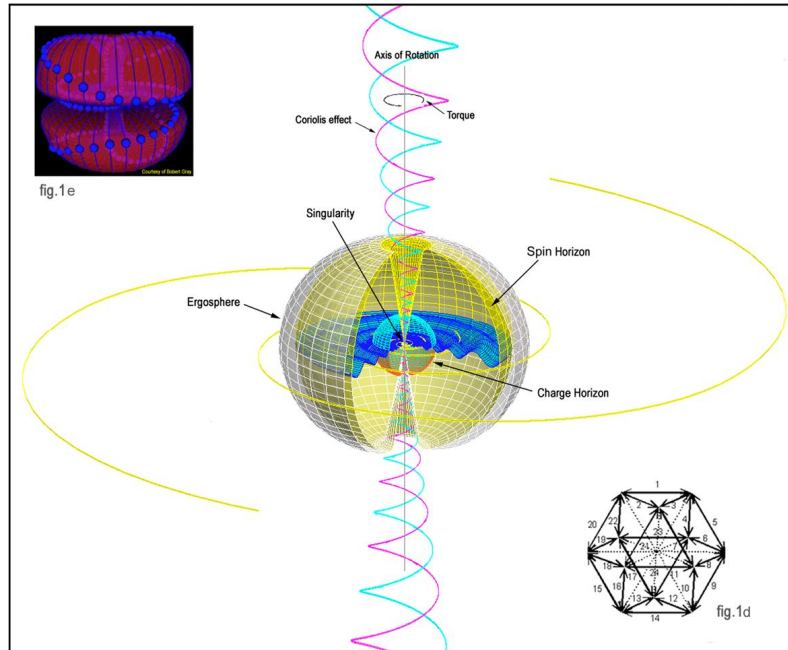


Figure 1(c)

Figure 1. The Lattice Universe, Kerr-Newman and Haremein Topologies

a) Lindquist and Wheeler dynamic universe utilizing a Schwarzschild-cell method [3] (from Lindquist and Wheeler Fig. 27.3) Many Schwarzschild zones are fitted together to make a closed universe. This universe is dynamic because a test particle at the interface between two zones rises up against the gravitational attraction of each and falls back under the gravitational attraction of each. Therefore the two centers themselves have to move apart and move back together again. The same being true for all other pairs of centers, it follows that the lattice universe itself expands and recontracts even though each Schwarzschild is viewed individually as static. This diagram taken from Lindquist and Wheeler (1957). b) Typical representation of a Kerr-Newman black hole (C. W. Misner, K. S. Thorne and J. A. Wheeler, Gravitation, Freeman and Co. (1973), p. 880). c) A schematic model of the N. Haremein toroidal topological membrane of a dual $U_1 \times U_1 \times U_1 \times U_1$ manifold and its singularity in a cuboctahedral field [2] (See Appendix A).

2. A SCALING LAW OF FREQUENCY VS RADIUS FOR BLACK HOLES

There appear to be different mass groupings of black holes. These categories of black holes fit well with the scaling model of Haramein [5, 6] and Rauscher [2, 4, 17]. The three main categories that astrophysicists have identified are, (1) “stellar” black holes, having a few times the Sun’s mass, (2) a mid-size black hole of perhaps 200 to $500 \times 10^4 M_A$ (3) “supermassive” black holes having a range of masses from 10^6 to $10^9 M_A$, at the center of galaxies and including quasars which are currently considered to be such black holes. However, the manner in which these systems, from supermassive to stellar black holes relate to each other, and certainly the manner in which micro physics relates is currently theoretically unclear. It may be that by describing all organized matter as various stages of evolution of black hole dynamics, and through the Haramein [5, 6] and Rauscher scaling law [2, 4, 13, 14], that these various systems can be related and understood to include microphysics as well. This will be discussed later in this paper.

We hypothesize that the characteristic frequency for the super giant black holes are of the order of, or less than, the characteristic frequency of the mid-size or intermediate black holes. We denote the mid-size black holes as G_1 and the super massive black holes as G_2 in our scaling law (See Figure 2a). Note that these systems are also x-ray emitters due to the plasma envelope surrounding them. We have developed a scaling law for the universal, galactic, stellar – solar and atomic scale frequencies with the consideration of a fundamental dynamical form of these systems within the Schwarzschild model. We plot fundamental associated frequencies, ω , vs. radius R of each of the systems (See Table 1. and Figure 2a).

In Figure 2a, we give the characteristic frequency and radius for each system derived from the Schwarzschild condition. We also give the mass for each system as well as the associated velocity, for verification of the model, which is approximately the velocity of light. In the figure we display an approximate plot of the various black hole systems. A more detailed analysis is currently in progress [14].

We find the scaling law fits the data on a linear-linear scale factor, which is significant. We start with the form $\omega = aR + b$ as a first order approximation. For the R intercept at $R = 10$ then $\omega \sim 8$. If $\omega \sim 0$ which can also be considered as 10^{-17} Hz, then for $R = 28$, we have $b/a \sim -1$. Thus we have the ω or Y intercept as (0, 8) and the R or X intercept as (8, 0) to a good approximation so that $\omega = -R + 8$. This law is derived from our graph utilizing dimensionless quantities for $c = 1$ from the relation $\omega \cong \frac{1}{t}$, $c = R/t$ so that $R\omega = c$ giving units $\omega = c/R$ and $R = c/\omega$. These are the dimensional conversion factors. Then $\omega = -R + 8$. In our graph we are using powers to the base 10 or plotting base 10 exponent factors. Hence we have $10^\omega \cong 10^{-R} + 10^8$ or $10^\omega + 10^R = 10^8$ so that $10^{\omega+R} = 10^8$. In this form we can take the log to the base 10 of both sides and return to our original equation $\omega + R = 8$ or $\therefore \omega = -R + 8$.

E. A. Rauscher calculates the evolution of physical parameters from a big bang universe, comprising a scaling law, which is consistent with the evolution under the constraints of a Schwarzschild universe [18]. Under the initial conditions of the big bang (as described by current theory), $\ell = 10^{-33} \text{ cm}$ and $t = 10^{-44} \text{ s}$ yields a frequency of rotation of 10^{43} Hz. Under the constraints of self consistency for its Schwarzschild condition, we have a rotational frequency of 10^{-17} Hz for the present universe.

In Figure 2a, we should mention that the form $10^{\omega+R} = 10^8$ is an approximation because of the variation in specific galactic and stellar systems. Also, we utilize the unit conversion of ω to R using $c=1$. We show this in Figure 2a. We can also write $10^{\omega+R} = 10^8$ using dimensional analysis in terms of a new vector quantity ω' and introducing a unit vector velocity as \hat{c} . Then we can write $10^{\omega+(\omega')^{-1}}$ where $\hat{c} = 10^8$ to also preserve proper dimensionality of our ω and R variables. We observe an approximate linear relation between R_s and M_s and also ω and R which is derived from fitting current astrophysical data. These fits utilize the first order Schwarzschild condition on astrophysical and cosmological systems as well as for atomic systems. In this approach we will analyze in detail the event horizon and ergospheric dynamics that will give us a more complete model of galactic and stellar formation and structure. Note that the expression which we derive here is a good first order approximation. Refinements, which include a more detailed formulation of black hole dynamics and other cosmological factors from general relativity, will include higher order effects in our scaling law.

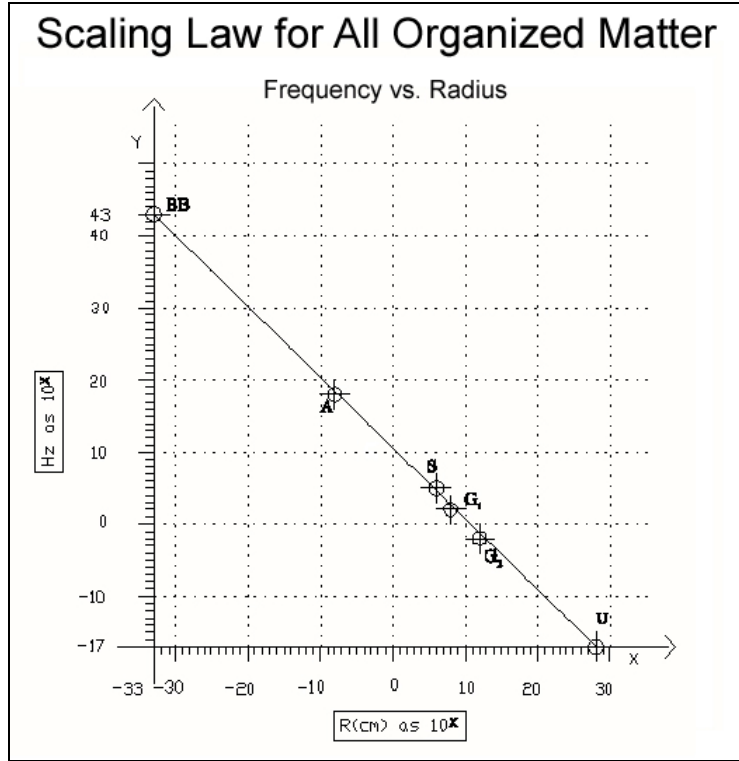


Figure 2a. A scaling law for organized matter of frequency vs. radius. The black hole system is presented in this figure. Plotted from the top left is the mini black hole at the Planck distance of 10^{-33} cm through to the stellar-sized black holes, larger black holes, galactic center black holes and at the lower right is a Universe-sized black hole. Note that in between the stellar size and the Planck distance mini black hole we have included a data point for the atomic size which we as well calculate a new value for its mass that includes the energy available in the vacuum space of a nuclei and yields the correct radius to describe an atomic resolution as mini black holes (see equation (5) to (18)) It is of interest that the microtubules of eukaryotic cells, which have a typical length of $2 \times 10^{-8} \text{ cm}$ and an estimated vibrational frequency of $10^9 \text{ to } 10^{14} \text{ Hz}$ lie quite close to the line specified by the scaling law and intermediate between the stellar and atomic scales [19].

System (cm/sec)	Frequency ω (Hz)	Radius R(cm)	Mass (gm)	Velocity C
Universe (U)	10^{17}	10^{28}	10^{56}	10^{10}
Galactic (G2)	10^2	10^{12}	10^{40}	10^{10}
Galactic (G1)	10^2	10^8	10^{36}	10^{10}
Stellar Solar	10^5	10^6	10^{33}	10^{11}
Atomic	10^{18}	10^{-8}	10^{-24}	10^{10}
Big Bang	10^{43}	10^{-33}	Unknown	10^{10}

Table 1. We list the associated radius, frequency, mass and velocity with various relevant systems. Plots of these values are given in Fig. 2(a) and 2(b). Note that the mass of the atomic resolution is given as the standard value (see the calculated value in equation (5) to (18)).

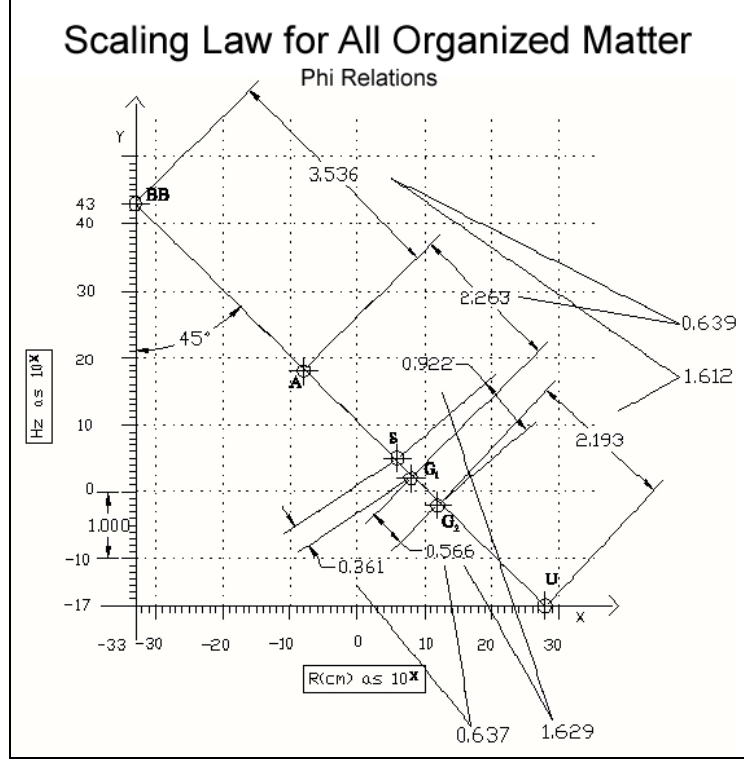


Figure 2b. We note that the distance between the data points on our graph, when divided with each other as in Figure 2b, yields a very close approximation to the familiar $\Phi(\phi)$ ratio given by $(1+\sqrt{5})/2 \approx 1.618$ and its inverse $(1-\sqrt{5})/2 \approx 0.618$. It is both appropriate and significant that the so called “golden ratio” is reflected in our scaling law (which maps energy dynamics at all scales), since it is prominently found everywhere in nature and has marked the evolution of cosmological mechanics and modern physics [18], from Kepler’s solar system modeling [20] to aperiodic Penrose tilings [21], including recent work on the thermodynamic phase transition of black holes showing a change of state from negative specific heat to positive specific heat at $(1-\sqrt{5})/2 \approx 0.618$ [22].

The linear progression of scale of organized matter in our universe from macro to micro, and their apparent coherent relationships, supports the structured vacuum hypothesis leading us to the description of its interaction and constraints on an event horizon topological spacetime manifold. Through black hole interactions with their surrounding plasma media, vacuum state polarization occurs and produces observable manifestations such as self coherent collective behaviors [4, 7, 16, 23].

If we consider the atomic resolution in our scaling law we find that it is the only one that does not obey the Schwarzschild condition. However, within the context of a polarizable vacuum where the quantum vacuum energy density is typically given as $\rho_v = 5.157 \times 10^{93} \text{ gm/cm}^3$ we can calculate the contribution of the vacuum energy necessary to produce a Schwarzschild-type condition for the nucleon radius. For a proton with a radius of 1.321 Fermi and a volume, V_p of $9.665 \times 10^{-39} \text{ cm}^3$, the quantity of vacuum energy available in the volume of a proton R_p is, $R_p = \rho_v \times V_p$, then

$$R_p = 5.157 \times 10^{93} \text{ gm/cm}^3 \times 9.665 \times 10^{-39} \text{ cm}^3 = \sim 4.984 \times 10^{55} \text{ gm/proton volume} . \quad (4)$$

One can calculate a similar result utilizing the proton volume V_p and dividing it by the Planck volume ℓ^3 equal to $4.220 \times 10^{-99} \text{ cm}^3$ extrapolated from the Planck length $1.616 \times 10^{-33} \text{ cm}$. This yields $2.290 \times 10^{60} \ell^3$ Planck volumes contained in a proton. A Planck’s mass being $2.176 \times 10^{-5} \text{ gm}$, it follows that the vacuum energy equivalent in a proton’s volume is

$$R_p = 2.176 \times 10^{-5} \text{ gm} \times 2.290 \times 10^{60} \ell^3 = \sim 4.983 \times 10^{55} \text{ gm/proton volume} . \quad (5)$$

Then we can calculate the proportion of vacuum energy available in the proton volume R_ρ to yield a mass M necessary for a nucleon to obey the Schwarzschild condition $R_s = \frac{2GM}{c^2}$ at the typical proton radius of 1.321 Fermi, then

$$1.321 \times 10^{-13} \text{ cm} = \frac{2 \times 6.674 \times 10^{-8} \text{ cm}^3 / (\text{gm s}^2) \times M}{8.988 \times 10^{20} \text{ cm}^2 / \text{s}^2} \quad (6)$$

where M equals the required mass,

$$M = \frac{8.988 \times 10^{20} \text{ cm}^2 / \text{s}^2 \times 1.321 \times 10^{-13} \text{ cm}}{2 \times 6.674 \times 10^{-8} \text{ cm}^3 / (\text{gm s}^2)} = \sim 8.898 \times 10^{14} \text{ gm} \quad (7)$$

provided from the vacuum density. It follows that only a very small proportion of the mass/energy available in the vacuum is necessary for a nucleon to reach the Schwarzschild condition since this ratio is

$$\frac{R_\rho}{M} = \frac{4.984 \times 10^{55} \text{ gm}}{8.898 \times 10^{14} \text{ gm}} = \sim 5.601 \times 10^{40}. \quad (8)$$

It is interesting to note that this ratio is approximately the ratio of the gravitational force to the “strong force” estimated to be 10^{40} times stronger than gravity. It then follows that only $1.785 \times 10^{-39} \%$ of the vacuum mass/energy available in the proton volume is needed to form a “Schwarzschild proton.” This contribution from the vacuum maybe the result of a small amount of the vacuum energy becoming coherent and polarized near and at the boundary of the spinning proton. A proton of such mass would produce a gravitational force acting on another proton situated at a diameter distance of

$$F = \frac{GM^2}{r^2} = \frac{6.674 \times 10^{-8} \text{ cm}^3 / (\text{gm s}^2) \times (8.898 \times 10^{14} \text{ gm})^2}{(2 \times 1.321 \times 10^{-13} \text{ cm})^2} = 7.570 \times 10^{47} \text{ dynes}. \quad (9)$$

We now calculate the velocity of two Schwarzschild protons orbiting each other with their theoretical centers separated by a proton diameter in this semi-classical approach. We utilize the force from Equation 9 to calculate the associated acceleration,

$$F = Ma \quad (10)$$

then

$$a = \frac{F}{M} = \frac{7.570 \times 10^{47} \text{ dynes}}{8.898 \times 10^{14} \text{ gm}} = 8.508 \times 10^{32} \text{ cm} / \text{s}^2. \quad (11)$$

We utilized this acceleration to derive the relativistic velocity as

$$v = 2\sqrt{ar} = 2\sqrt{8.508 \times 10^{32} \text{ cm} / \text{s}^2 \times (2 \times 1.321 \times 10^{-13} \text{ cm})} = 2.998 \times 10^{10} \text{ cm} / \text{s}. \quad (12)$$

We obtain $v = c$, then the period is

$$t = \frac{2\pi r}{v} = \frac{2 \times 3.142 \times (2 \times 1.321 \times 10^{-13} \text{ cm})}{2.998 \times 10^{10} \text{ cm} / \text{s}} = 5.537 \times 10^{-23} \text{ s} \quad (13)$$

which is the characteristic of the interaction time of the strong force. The strong interaction manifests itself in its ability to react in a very short time. (For example, for a particle which passes an atomic nucleus of about 10^{-13} cm in diameter with a velocity of approximately $10^{10} \text{ cm} / \text{s}$, i.e. with a kinetic energy of $\sim 50 \text{ MeV}$ for a proton and 0.03 MeV for an electron, the time of strong interaction is about 10^{-23} s). [24] The frequency calculated from equation (13) is then

$$f = \frac{1}{T} = \frac{1}{5.537 \times 10^{-23} \text{ s}} = \sim 1.806 \times 10^{22} \text{ Hz} \quad (14)$$

which is within the gamma ray emission frequencies of the nucleus of an atom. This is a remarkable result.

We next compare these calculated gravitational forces between two Schwarzschild protons to the strong force generally used to account for their attraction. The strong force coupling constant is considered to be 1 and on this scale the relative electromagnetic coupling constant is $\alpha \sim \frac{1}{137}$. The strong force can be approximated as the Coulomb repulsion strength multiplied by the inverse of the fine structure constant, 137. Then the repulsion of two protons just touching is

$$Force = \frac{Kc q_1 q_2}{r^2} \quad (15)$$

where $Kc = 8.988 \times 10^9 Nm^2C^{-2}$ and $q_1 = q_2 = 1.602 \times 10^{-19} \text{Coulomb}$ which is the charge of the proton. Then

$$F = \frac{8.988 \times 10^9 Nm^2C^{-2} \times (1.602 \times 10^{-19} C)^2}{(2 \times 1.321 \times 10^{-15} m)^2} = 33N \text{ or } 3.3 \times 10^6 \text{ dynes} \quad (16)$$

yielding an estimated strong force between them of $3.3 \times 10^6 \text{ dynes times } 137 \text{ which equals } 4.52 \times 10^8 \text{ dynes}$ at a separation where the two protons are contiguous. It is clear from these results that the “strong force” may be accounted for by the gravitational attraction between two Schwarzschild protons as calculated in Equation (9). Most of the gravitational component, including a portion of the vacuum energy, may be utilized for confinement at the quark resolution.

As seen above the vacuum polarization may have an important role to play in micro and macro scale energetic processes. In recent years the vacuum energy density has been measured by various international and American university laboratories [25, 26, 27, 28, 29]. At the universal level, the necessity to reinstate the cosmological constant to accommodate the accelerating expansion [30, 31] is evidence that this energetic vacuum has physical properties and is acting at all scale levels, and may indicate a universal rotation. Thus, the vacuum can be described in terms of gradients between scales of density of mass-energy (as in our scaling law) producing various rotational rates. For instance, the density of intergalactic vacuum relative to the galactic internal density, or the density changes near the surface of the event horizon of the centering black hole of a galaxy, where particles accelerate toward the velocity of light, generates various gradient differentials driving angular momentum/spin at all scales. These different density scales interact to generate topological boundaries, from which the scaling law can be derived. Thermodynamic and electrohydrodynamic Coriolis type processes on the surface of these event horizon boundaries are a consequence of this vacuum density gradient, not unlike the high pressure and low pressure differential in the air plasma of our atmospheric turbulences producing significant energy events such as hurricanes, lightning storms and tornados. Moreover, the prevalent structure of subatomic particles, and the highly ordered arrangements of superclusters [9, 10] are indications of a structured vacuum [4]. Further, we examine cosmological, galactic, stellar, and atomic level black holes, and a new approach to the early universe big bang solutions is briefly discussed.

3. STELLAR SIZE BLACK HOLES, A NEW UNIVERSAL SCALING LAW AND THE ROLE OF THE VACUUM STRUCTURE

Our current model of cosmogenic and cosmologic evolutionary physical parameters deals with the universe as a whole. Even in these relatively simple approximations, we observe non-linear cosmogenic effects in analogy to the inflationary models, and we complement it with a continuous scale at the micro physics level with some of the preliminary work presented in this paper [18]. The Hubble cosmological constant now becomes an approximation for distant cosmological regions of space where large red shifts are observed.

The galactic center black hole systems, which have been hypothesized to exist for well over two decades, and for which there is a great deal of observational evidence, must occupy some role in the nature and structure of the whole galactic system [1]. They have been observed to be associated with the center of most galactic disks that have been analyzed, and it is appropriate to assume that these gigantic black holes occupy an important role in galactic formation and dynamics. We briefly address the topological details of these fields, which are related to the vacuum structure in the next sections, but the N. Haramein double toroid topology depicted in Figure 1b is a representation of the field dynamics solution we are using for each scale (see reference 2). The toroidal topology is a central feature of the Haramein [5, 6] and Haramein-Rauscher model [2, 4, 14] briefly described here and detailed in reference [2]. Further, if we consider Planck length mini black holes at the micro level, we may contemplate the possibility of the same field dynamics in the quantum domain. In the next sections, we introduce some astrophysical

observations and theoretical concepts which we believe will lead to a better understanding of the universality of the black hole structure and its relation to the vacuum phenomenon.

In order to appropriately discuss the dynamics of a collapsing stellar object, one must first address the issue of gravitational collapse and its global consequences. Of course, a detailed analysis is outside the scope of this paper, and only a brief overview addressing the challenge of extreme curvature will be given, with further details in future publications. Misner, Thorne and Wheeler described the evidence of gravitational collapse provided by stars and the universal big crunch “as the greatest crisis in physics of all time” [32]. Schwarzschild’s solutions to Einstein’s field equations, which lead to the extreme curvature of singularity, were the first solutions found, and were presented by Einstein in 1916. As the result of gravitation, the universe expands to a maximum dimension then re-contracts and collapses to singularity, and then nothing, no more predictions are made, and Einstein’s field equations invariably develop singularity [12]. Further, at the quantum resolution, the vacuum fluctuations are so great (formally infinite) that they were renormalized utilizing the Planck scale. The topology fluctuates inducing wormhole-like structures at the Planck distance (quantum foam), thereby generating a gravitational collapse which is continually being formed and unformed everywhere in space. It has been remarked that the Planck distance quantum fluctuation could be “a guide to the outcome of collapse at the level of a star and at the level of the universe” [33]. In the 70’s evidence of the possibility of a collapsing dynamic generated a large conceptual challenge or a paradox – since below singularity no physics can be, or has been described, “yet physics surely continues to go on” [32].

Currently we have very strong observational evidence of collapse at stellar, galactic and quasar scale. Further, the vacuum fluctuation density of the quantum resolution, which has gained great support from theory and experiments [25-29], is evidence that collapse may be occurring at the subatomic particle level producing a polarized structured vacuum. Certainly, if the universal scale emerged from singularity and returns to singularity, and gravitational collapse is found at the star and galactic center resolution, and finally, if we find that collapse as mini black holes is occurring everywhere in space in a dynamical vacuum, then one can deduce that collapse is not only predicted by the high curvature of the metrical space, but that it is fundamental to the spacetime manifold topology as it interacts with matter/energy.

In view of the Lindquist and Wheeler [3] dynamical universe collapsing and expanding, and that singularity may be occurring at all scales, a white hole (expansion) centered by the singularity of a black hole (collapse) would be expected. It follows that the singularity horizon may no longer be smooth, and the “black hole has no hair” analogy may no longer hold. The Lorentz invariance condition is dealt with by utilizing the U_4 bubble so that the hairs may be combed uniformly along the torodial topology without the necessity of a “part” [2]. Further, these spacetime topological hairs undergo specific Newtonian-type gyroscopic and Coriolis dynamics that are typically observed in plasma and their self-organizing structures and which are associated with strong electromagnetic radiation (the white hole expanding portion) found in ergospheres and multiple astrophysical bodies. One could even think of the arms of a galaxy as the very long “hairs” of the central black hole ergosphere and bulge. New data from black holes such as the one at the galactic center of MCG-6-30-15 have now been observed to radiate generous amounts of luminous emissions, which can not be accounted for by the free falling matter alone [34, 35]. In Laplace transformation, space and time are not limiting cases but effect orientation.

In the world of a structured white holes/black holes “dimpled” universe, unification is given by a topological scaling defining horizons at all scales – where the micro physics is dealt with as high curvature near the Planck distance of mini black/white holes and the large scale is quantized by “hairy” horizons. A condition of equivalence resulting from the dynamic-balance between the electromagnetic radiation and the collapsing geometry of space can be written and a first consideration is given in reference [4]. In the black hole/white hole dual structure, the singularity may occupy a role in a mirror inverse where mass-energy is destroyed and recreated by the fundamental torquing of spacetime.

If we consider the topology of infinite curvature in a spacetime manifold (with the inclusion of torque, Coriolis effect and charge [2]) of a white hole containing a collapsing black hole singularity, the relationship between the weak gravitational field (the white hole portion) and the highly curved space at the center singularity, generates a spacetime topology equivalent to a $U_1 \times U_1$ torus and its polarized Coriolis counterpart resulting in a $U_1 \times U_1 \times U_1 \times U_1$ double torus. Thereafter, when one examines the radius as it approaches zero at singularity, one finds the vacuum since the torus topology is centered by a hole. Vacuum fluctuations may be caused by the extreme curvature pinching the vacuum structure at the center of black holes at all scales where mass approaches infinity and where the vacuum is renormalized as 5.157×10^{93} gm/cm³ at the Planck resolution [2, 4].

Hawking compares the vacuum quantum foam fluctuation to electron-positron pair production, and states that “*whether spacetime has a manifold structure on these scales [quantum foam] is open to question. It is hypothesized that this structure might be a fractal structure. But manifolds are what we know how to deal with,*

whereas we have no idea how to formulate physical laws on a fractal” [36]. At the Planck scale, at the center of the dual torus, collapse must assume the minimum amount of vector symmetry for ideal equilibrium of all forces so that they may sum to zero and appear as vacuum. In reference [2] and in some detail in Appendix A, we expressed how the subset of the cover group $U_1 \times SU_2 \times SU_3$ containing the cuboctahedron is utilized and related to the group set of the dual torus $U_1 \times U_1$. At the vacuum resolution, vacuum structure must converge to the minimum vectors for equilibrium – the twelve converging vectors of a cuboctahedron. The fractional problem generated at singularity and, thus, at the vacuum may be resolved by the fractalization of the twelve collapsing vectors necessary for minimum equilibrium of the cuboctahedral growth of a structured vacuum – a 3D Koch-type curve, from which one can find resolutions of structures to infinite discreteness. This may be a viable method to apply fractal geometry to the spacetime manifold, and to use fractal resolutions to scale singularity.

The vacuum density gradient, $\nabla^2 \phi = 4\pi\rho$ where ρ represents the renormalized gradient and ϕ its potential so obtained, relates to our scaling law, which extends from the Planck length to the Universe as a whole, and the variation in density dictates the energy level of the vacuum at various scales. From the work of Hamein and Rauscher [2], we consider, for instance, at the cosmological constant $\Lambda \neq 0$ where the energy density of the vacuum is

$$E = \left(\frac{c^5 \hbar}{G} \right)^{\frac{1}{2}} = 1.25 \times 10^{16} \text{ ergs} \quad (17)$$

for a universal acceleration of

$$a = \left(\frac{c^7}{G\hbar} \right)^{\frac{1}{2}} = 5.73 \times 10^{53} \text{ cm/sec}^2 \quad (18)$$

at the lower limit of

$$\ell = \left(\frac{G\hbar}{c^3} \right)^{\frac{1}{2}} = 1.62 \times 10^{-33} \text{ cm} \quad (19)$$

where the energy density is

$$\rho = \frac{c^5}{G^2 \hbar} = 5.16 \times 10^{93} \text{ gm/cm}^3 \quad [13]. \quad (20)$$

The cosmological constant is expressed in Einstein’s field equations as

$$R_{\mu\nu} - \frac{1}{2} g_{\mu\nu} R_{\mu\mu} - \Lambda g_{\mu\nu} = \frac{8\pi G T_{\mu\nu}}{c^4}. \quad (21)$$

The difference in vacuum density and thus the difference in the amount of Fermi-Dirac sea of interactions of creation and destruction operators [7], drives the continuous dynamic collapsing and uncollapsing manifold topology at all scales. This is analogous to the interaction of high density and low density air pressures generating and driving the magnetohydrodynamic plasma topology of hurricanes and tornados, in this case, however, driving the toroidal topological manifold of white/black hole structures at all scales. The differential in density between the external vacuum and the internal black hole vacuum may be the cause of vacuum polarization type of processes at the event horizon, responsible for pair production of mini white hole/black holes.

Note that recent background radiation data collected by the Wilkinson Microwave Anisotropy Probe indicates a quite different picture of the topology of the universe than previously believed; one that seems to be toroidal in nature [37]. The CMB mapping octopole and quadruple components exhibit a particular spatial axis of polarization with a highly structured equator, supporting the dual torus topology being present at least 400,000 years after the big bang when the extremely hot hydrogen plasma was fully ionized. We compare these findings to the mapping of galactic structures and to the dynamics of the plasma in supernova events where large departures from the typical spherical models is necessary, and is a match to the dual torus topology [38]. The same structures are, as well, observed at the collapsed star, the microquasar and quasar resolutions. Further, it appears that the distribution at the very large scale of superclusters seem to self-organize at the vertices of octahedrons, generating an immense latticework of cuboctahedrons [9, 10].

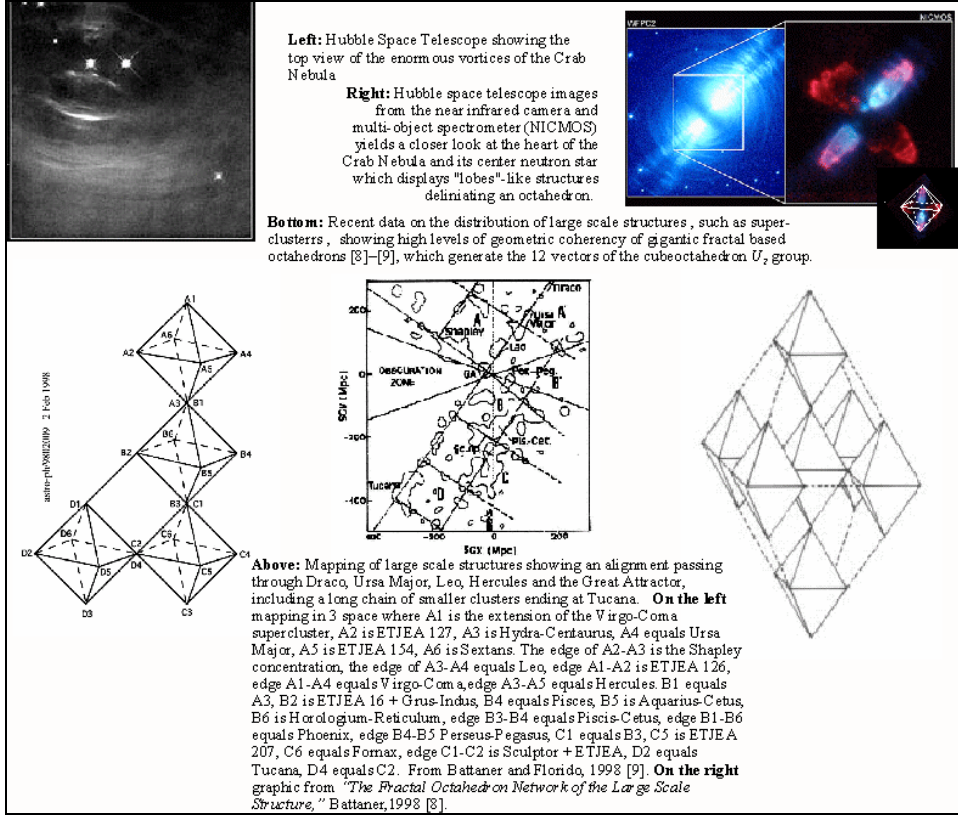


Figure 3. Large scale structures

- (a) Hubble Space Telescope image showing the top view of the enormous vortices of the Crab Nebula.
- (b) Hubble Space Telescope images from the near infrared camera and multi-object spectrometer (NICMOS) yields a closer look at the heart of the Crab Nebula and its center neutron star which displays "lobe-like" structures delineating an octahedron.
- (c) Mapping of large scale structures showing an alignment passing through Draco, Ursa Major, Leo, Hercules and the Great Attractor, including a long chain of smaller clusters ending at Tucana.
- (d) Recent data on the distribution of large scale structures, showing high levels of geometric coherency of gigantic fractal-based octahedrons [9, 10] which generate the 12 vectors of the cuboctahedron U_2 group. (See also Fig. 3(d). This is a mapping in 3 space of the data of Figure 3(c) where A1 is the extension of the Virgo-Coma supercluster, A2 is ETJEA 127, A3 is Hydra-Centaurus, A4 equals Ursa Major, A5 is ETJEA 154, A6 is Sextans. The edge of A2-A3 is the Shapley concentration, the edge of A3-A4 equals Leo, edge A1-A2 is ETJEA 126, edge A1-A4 equals Virgo-Coma, edge A3-A5 equals Hercules. B1 equals A3, B2 is ETJEA 16 + Grus-Indus, B4 equals Pisces, B5 is Aquarius-Cetus, B6 is Horologium-Reticulum, edge B3-B4 equals Piscis-Cetus, edge B1-B6 equals Phoenix, edge B4-B5 Perseus-Pegasus, C1 equals B3, C5 is ETJEA 207, C6 equals Fornax, edge C1-C2 is Sculptor + ETJEA, D2 equals Tucana, D4 equals C2. (From Battaner and Florido, 1998 [10].
- (e) Graphic from "The Fractal Octahedron Network of the Large Scale Structure", Battaner, 1988 [9]

4. SPIN HORIZON

We are defining a novel form of horizon which we term the "spin horizon," or the "SH" boundary condition, based on the rate of spin and acceleration of various bodies as the radius approaches zero in a torquing spacetime Hamein-Rauscher solution. The horizon is defined where torque approaches zero, $\tau_{\mu\nu} \rightarrow 0$ and the circular velocity approaches infinity, $v_c \rightarrow \infty$. While the original Schwarzschild radius was derived based on a stationary body, it is observed that all bodies are spinning. Recent studies now show that black holes spin and, in fact, it is now found that galactic supermassive black holes may spin near the speed of light [39, 40].

Traditionally, it has been thought that only stars above three solar masses can form singularities after going nova. Should a spin event horizon be established, singularities or singularity-like structures may be demonstrated to exist in all organized matter. In this view the white hole/black hole duality is present from cosmogenesis in a continuous creation and annihilation, contracting-expanding, universe. In what follows, we express our solar dynamics in those terms and demonstrate a self-similarity of the Sun to the galaxy which have fast-spinning supermassive black holes at their centers.

a) Galaxies spin too fast

A long-standing puzzle of galaxy behavior is the speed of their rotation. Most estimates of their masses based on visible luminous matter conclude the galaxies are spinning too fast for their estimated mass and by Keplerian celestial mechanics, are spinning above escape velocity at all regions from their bulges to their discs. According to such analysis they should all fly apart. How do galaxies remain as organized systems rather than dissipating as their matter escapes?

Also galactic disc regions rotate at approximately the same speed from just outside the bulge out to their visible edges, thereby rotating as if they were nearly solid bodies. Again, by Keplerian analysis, rotation rates should fall with increasing distance by $1/r^2$. This “flatness” of their rotation curves and the “extra mass” purported to account for the stability of the galaxies is currently explained by the hypothesized presence of spherical “dark matter” halos that account for the so-called “missing mass”. (See Figure 4.) Yet after some 70 years of looking, we have yet to observe “dark matter”. In fact, it is recently reported that elliptical galaxies show little or, perhaps, zero “dark matter” [41] and as suggested in one article [42], this means that “some of the missing matter is missing”.

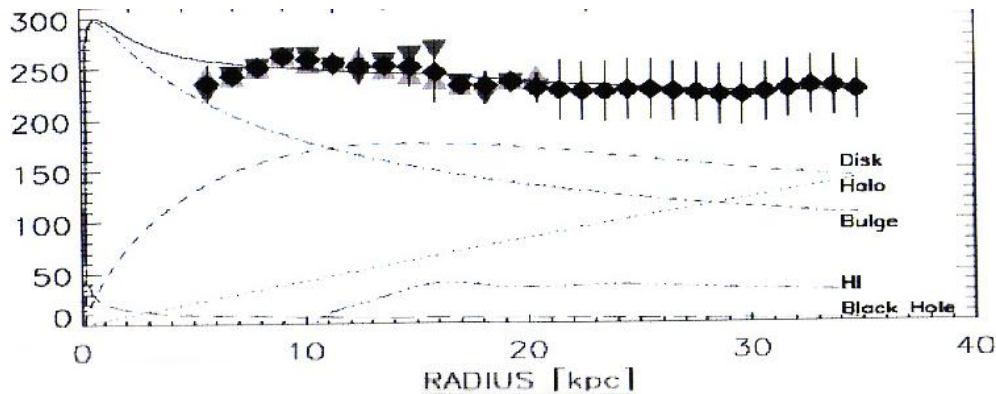


Figure 4. Rotation rates vs distance from the center for the galaxy M31
The various curves denote the supposed contribution to the total rotation of the central black hole, hydrogen, the bulge, the dark matter halo and the disk masses.

An alternative approach may be to assume that our calculations are the ones missing something. This issue may be resolved by proper accounting of the origin of spin [2], currently thought to have originated in the big bang, and conserved ever since in some ideal frictionless environment. In a spacetime which incorporates a source of angular momentum in the stress energy tensor, such as a torque producing a Coriolis torsion dynamic on the metrical space, and assuming a viscous media, galactic structures, the plasma dynamics of ergospheres and stars atmospheric behaviors may be best described by magnetohydrodynamics (MHD) driven by the structure of spacetime itself. In these conditions shear layers such as Hartmann layers and others define specific horizon conditions that may appropriately elucidate the so-called galactic flattening problem. Furthermore, as the radius of a system reduces, the torquing of spacetime in a Hamein-Rauscher metric produces an increasing angular acceleration with particle velocities tending towards c at a very specific radius – the spin horizon. In this section, we demonstrate the derivation of the spin horizon for our Sun using galactic scaling relationships.

b) Many Rotating Systems are Self-Similar

Spinning systems at various scales show similar characteristics, namely, a flattening of their rotation curves, including galaxies, our Sun, and hurricanes. (See Figure 5). Tornadoes are similar vortex structures with luminous phenomena, gamma ray emissions and other behaviors which have been suggested to arise from a polarized structured vacuum. [43, 44, 45, 46, 47] Qualitatively, these structures are similar despite great disparity in size. In Figure 5, we demonstrate that the Sun’s MHD, at an average density of 1.4 that of water or even hurricanes with an average density of 1.7×10^{-5} that of water exhibit the same characteristics such as the so-called “galactic flattening,” found in galactic structures which have an average density of 1 particle per meter. It is uncanny to find as well that the Sun’s core and the galactic bulge both represent 0.2 of their respective radii. These results express that common mechanisms may relate the spin dynamics of MHD at all scales.

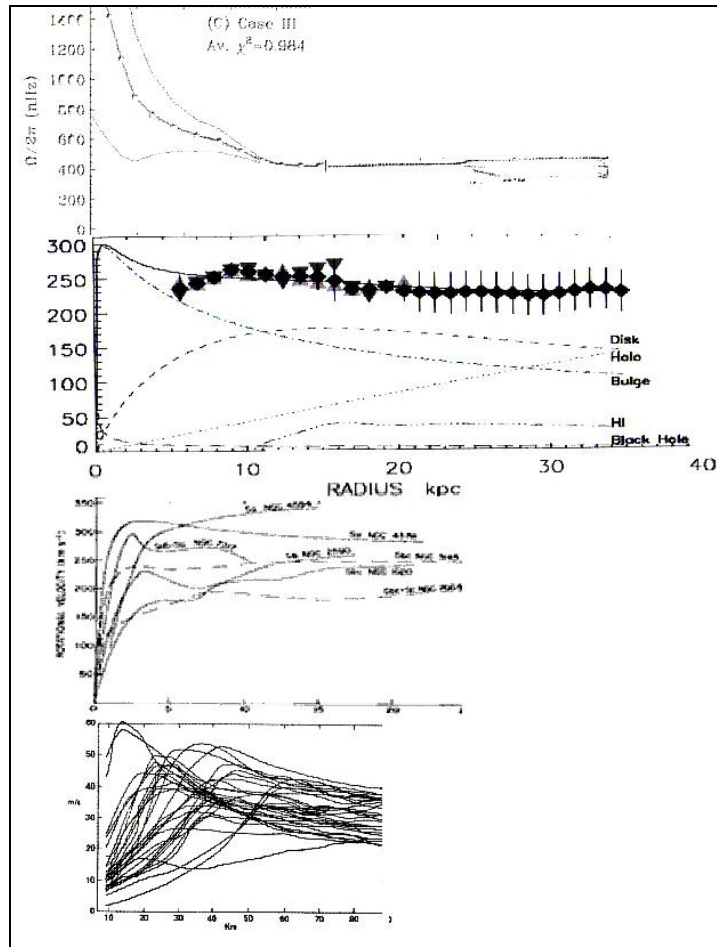


Figure 5. Self-similarity of the Sun, galactic and hurricane rotation curves
 a) Rotation rate profile of the Sun; left half [48], right half [49] b) Rotation rate for M31[50]; c) A collection of various galactic rotation curves; d) Various hurricane rotation rate curves [50] Evidence that the central black holes are spinning rapidly comes from Yoshiaki, and Rubin [51] and Y. Sofue et al.[52] who show by observations of the carbon monoxide (CO) lines, that the inner bulge of galaxies with the clearest evidence of a central super-massive black hole, when plotted on a log scale (see Fig. 6), show the bulge rotation is Keplerian, in the case of the Milky Way galaxy, from the center out to 0.001 of its total radius. Beyond this, there is a clear flattening of the rotation curve.

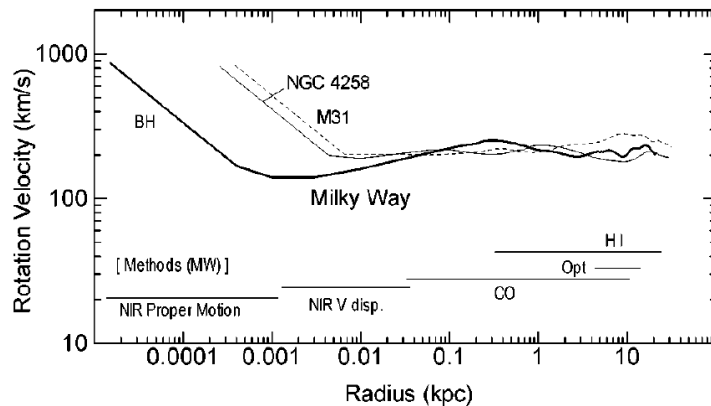


Figure 6. Logarithmic plot of Galaxy Rotation Rates. Note that the bulge is Keplerian, only outer curves are “flattened”

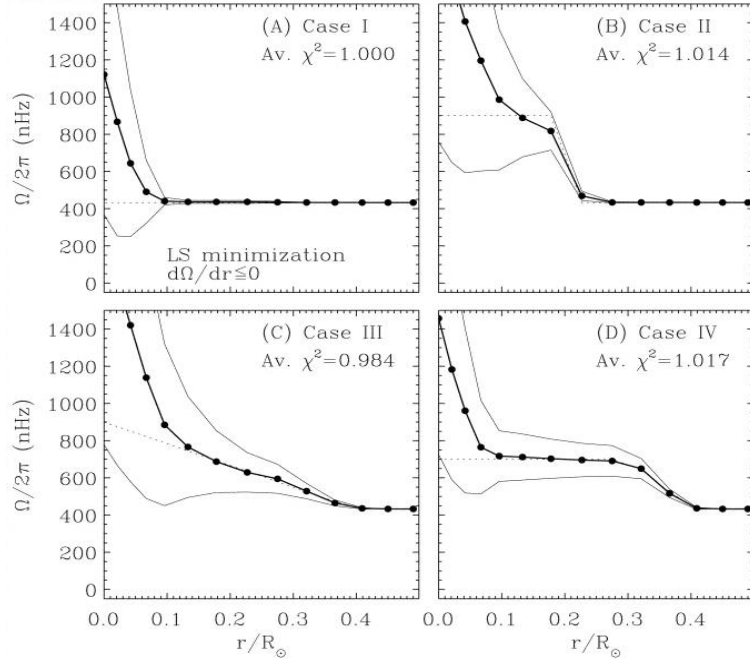


Figure 7. Sun Rotation Rate from Helioseismology Predictions: Genetic forward modeling of the rotation near the core of the Sun. We use Case III above as our model for the rate of rotation of the Sun [48].

c) A Spin Event Horizon for the Sun

Charbonneau, et al. used a genetic forward modeling approach to estimate the interior rotation rates of the Sun near its core. Their conclusion is that the Sun's rotation rate is likely flat down to 0.1 of its radius. However, in their Case III they fit the data assuming a monotonically increasing rate. See Figure 7. We have used this estimate to derive the radius of a spin event horizon for the Sun. Figure 8 shows an estimated Sun rotation curve from the center, 0 out to 100% of its radius.

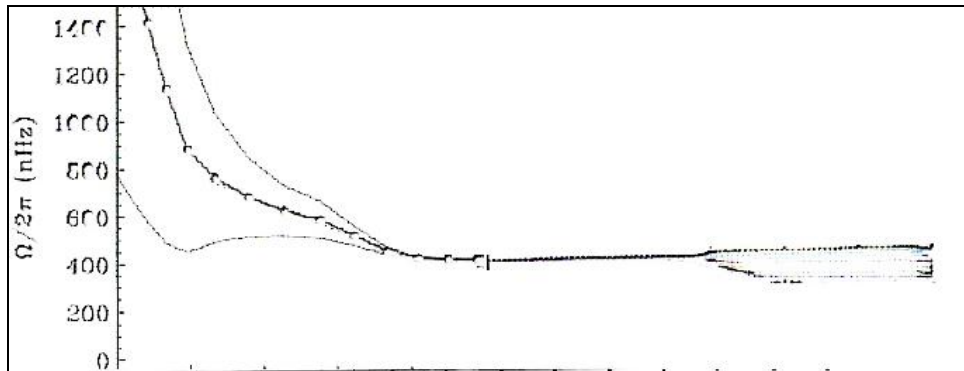


Figure 8. Sun Rotation rates Rotation rate (in nano-Hz) vs radius (0.0 to 1.0) for the Sun after references [48, 49] Note similarity to galactic rotation curves. In the outer part, rotation frequency depends on the latitude, shown by the spread of curves seen toward the right. The period is 24 days at the equator, and about 32 days near the poles (approx 400 nHz).

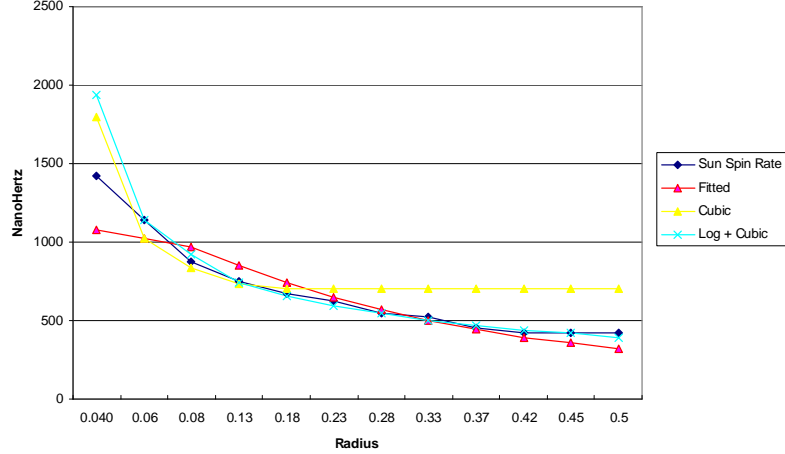


Figure 9. Speed of rotation vs Radius extrapolated to light speed, c . A log plus cubic curve was fitted to the estimated rotation rates [48] for the inner core of the Sun and extrapolated to estimate where rotation rate reached c , the radius of a *spin horizon of the Sun* of about 220 Km.

We fitted a log plus cubic curve to the estimated rotation rates [48] for the inner core of the Sun and then extrapolated this curve inward to find where the estimated rotation rate reached c , the radius of a *spin horizon of the Sun*. The result was a *spin horizon* radius of about 220 Km. See Figure 9. Fitting a similar curve to the lower and upper bounds shown for Case III yielded a minimum estimate of 140 Km radius and a maximum radius of 350 Km.

Next, we estimated the mass of the Sun's putative *spin horizon* "singularity" assuming the self-similarity of the Sun with the galactic scale. We used a scaling law for galaxies and the size of their central black holes derived by Farrarese [53] from a sample of 16 spiral and 20 elliptical galaxies, where the bulge velocity dispersion σ_c , is found to correlate tightly with the galaxy's circular velocity v_c , the latter measured where the rotation curve is flat. The mass of the central black hole of a galaxy is given as...

$$M_{\bullet} = (1.66 \pm 0.32) \times 10^8 (\sigma_c / 200 \text{ Km s}^{-1}) 4.58 \pm 0.52 M_A \quad (22)$$

From the rotation velocities of Case III, we derive a dispersion which is defined as the standard deviation of the rotation velocities of the bulge of the galaxy [53]. The dispersion of the Sun is then calculated utilizing the rotation velocities of its core (which is analogous in percentage of size to the galactic bulge as mentioned above), resulting in $\sigma_c = 0.375964779$. Substituting this value in equation (22), we estimate that the central "*black hole-like structure*" for the Sun, analogous to the center of our galaxy, is equal to 5.439×10^{-5} the mass of the Sun or about $1,082,474 \text{ Kg}$ or $1.082474 \times 10^9 \text{ gm}$ and represents some $5.439 \times 10^{-3} \%$ of the mass of the Sun, utilizing a low estimate of the dispersion.

Farrarese [53] also gives a relationship between the dispersion of the bulge velocities and the circular velocity of the disc of a galaxy:

$$\text{Log } v_c = (0.84) \text{ Log } (\sigma_c) + 0.55 \quad (23)$$

Again, using a velocity dispersion of $\sigma_c = 0.375964779$ for the Sun, we can derive the circular velocity of the Sun based on equation (23). We find this value is $\sim 1.887 \text{ Km/sec}$ or $1.887 \times 10^3 \text{ cm/sec}$. The actual circular velocity of the Sun can be calculated from its estimated period of 26 days at the equator, with a radius of $\sim 675,000 \text{ Km}$ or $\sim 6.75 \times 10^8 \text{ cm}$, the circumference of the Sun is $\sim 4,239,000 \text{ Km}$ or $\sim 4.239 \times 10^9 \text{ Km}$. Twenty-six days is $\sim 2,246,400$ seconds. Then the circular velocity is $\sim 1.5599 \text{ Km/sec}$ or $\sim 1.5599 \times 10^3 \text{ cm/sec}$. The actual value is $\sim 1.88 \text{ Km/second}$ or $\sim 1.88 \times 10^3 \text{ cm/sec}$ and is a remarkably good match to the value obtained. This is significant considering that the Sun is approximately 11 or 12 orders of magnitude smaller than the Milky Way.

A better fit may be found. Since the Sun's estimated period varies from 23 days to 28 days, repeating the calculation with the 28 day period yields 1.7522 cm/sec which represents only a 12% error over approximately 11 orders of magnitude. This calculation is supportive of our scaling law presented in Section 2. that characterizes matter at all scales as self-similar "black hole-like" phenomena. Further, as in the galactic scale where a central black hole is found and where data is now showing velocities approaching c , our Sun may host a similar

singularity-like structure at its center, with a flat rotation curve similar to spiral galaxies, and a circular velocity well predicted by its dispersion.

Our local stellar object, the Sun, is a complex acoustical oscillator, from which the analogy of a sounding bell can be derived. The plasma dynamics of the Sun are consistent with stellar and galactic observable plasma excitation modes, and their toroidal field topology. Some of these modes of dynamic plasma oscillations are plasmon-acoustic, and may explain the solar dynamic turbulence as well as observed plasma dynamics surrounding known black holes, such as galactic centers, mid-size and stellar black holes [4]. Thus, our Sun's ergosphere exhibits some of the dynamics we would expect in the vicinity of the horizon of a black hole including that it is a significant x-ray emitter. The similarity in these plasma dynamics and its field topology, found at all scales, may be a strong indication of the validity of the above approach to the energy dynamics at the inner structure of our local star, and the resulting angular momentum of our solar system. When we examine the modes of excitative oscillations, we find that they could be described by a hollow core circumscribed by the semi-permeable spin horizon of a black hole-like structure generating plasmon acoustic excitation of the ergosphere as matter plunges across the horizon—where a resonance cavity is consistent with acoustic oscillating modes, just as an empty bell resonates better than a full one. Sunspot-type activity may be found upon closer examination of stellar, galactic and quasar black hole ergospheres as well.

One of the predominant features of the Sun is the periodic sunspot structures that appear on its surface, the source of which has not been well understood to date. Using the above white hole/black hole concept, Hamein hypothesized a decade ago that these breaks in the plasma dynamics were not only surface events, but were caused by the internal gravitationally collapsing structure absorbing material and generating immense vortex-like Coriolis dynamics swirling plasma towards the solar center. In recent findings gathered by SOHO, the extreme UV data indicates that sunspots have been shown to be enormous plasma hurricanes that occur beneath the stormy surface and are sucking in material towards the center of the Sun [54], where previously they were thought to be surface events only and expelling material. It is important to note that the sunspot regions are extremely high x-ray emission areas, which would be expected in regions where matter spirals inward towards center. The observation that sunspots appear to commonly have antipodes suggests as well a highly polarized plasma structure. The plasma dynamics of our atmospheric environment are similar to the ones observed in the plasma dynamics of the ergosphere of our Sun.

CONCLUSION

From the recent data and some current theoretical considerations, we have developed a scaling law from macroscopic current universal black holes, to galactic, stellar and mini black holes, which obey the Schwarzschild condition and the Kerr-Newman metric, extending the scale topology to the microphysics of the Planck distance. In recent years, observational black hole physics has become a dominant feature of astrophysical considerations. After more than fifty years of theoretical models, we now have a variety of observations of black holes at various scale levels, from stellar, to galactic and cosmological phenomena, and we observe that all resolutions have very similar plasma dynamics, (all of them are x-ray emitters), and similar field topology characteristics. These exciting observations have led to theoretical and experimental advancement in order to better describe the state of a black hole, which extends to the vacuum state virtual interactions. Further, we demonstrate that a polarized vacuum structure may be intimately involved in the dynamics of formation of black holes from the atomic resolution to universal size defining similar mechanics at all scales. These polarization structures seem to be consistent as well with the Hamein-Rauscher metric producing dual torus U_4 concentric white hole/black hole dynamic and its harboring cuboctahedral singularity and is consistently observed in various astrophysical data. We briefly discuss an energetic structured vacuum at Planck distance, utilizing a cuboctahedral fractal Koch curve at singularity.

The basic condition of the relationship between black holes and the vacuum is at the atomic scale level, where we relate the strong nuclear force to the gravitational force within the Planck black hole. The form of the cosmological and mini black holes coupling to vacuum state polarization is hypothesized to give rise to the recent observations of the scale size and the form of black holes and other astrophysical features. In the later sections we are able to scale the dispersion of the bulge velocity derived from galactic structures and apply them to our Sun with remarkable accuracy considering the scale magnitudes. This again points to the dynamics of similar mechanics involving black hole structures at all scales. The development of the scaling law will allow for a better understanding of organized matter in the universe and give us a uniform and unified picture of the dynamics of physical laws acting on various scale systems, and thus, a unified model.

Acknowledgements

The authors wish to express their gratitude for the support and fellowship of our colleagues at The Resonance Project Foundation. Also, we express particular appreciation to S.P. Sirag for fruitful discussions.

Appendix A

The fundamental topology of the vacuum is presented and the analysis of the specificity of the existence of specific elementary particle properties which are generated and observed. We also apply this topological structure to the analysis of macroscopic cosmological structures. In this Appendix we elaborate on the topology presented in the previous section. First we present some background on group theory and then the model.

The special unitary Lie groups, which are topological groups having infinitesimal elements of the Lie algebras, are utilized to represent the symmetry operations in particle physics. For example, the generators of the special unitary, SU_2 group is composed of the three isospin operators, I as I_x , I_y and I_z having the commutation relations $[I_x, I_y]=iI_z$. The generators of SU_3 are the three components of I spin and hypercharge, Y and for other quantities which involve Y and electric charge, Q . Thus, there are eight independent generators for the traceless 3×3 matrices. The O_3^+ group of rotations is homomorphic to the SU_3 group.

The regular polyhedral groups, includes the cube and octahedron as the 24 element octahedral group. The octahedral group is a finite subgroup of the Lie group SO_3 and the octahedral double group is a subgroup of SU_2 . Corresponding to the continuous Lie group SU_2 acts on a two dimensional real space in analogy to SO_3 acting on a three dimensional real space. Significantly, S^3 group, also called the SU_2 group acts as a space which is the double cover of SO_3 because SU_2 as a space is a sphere S^3 , SO_3 which is $S^3 / \{ \pm 1 \}$ so that SO_3 can be derived from SU_2 by the plus and minus elements of SU_2 in order to form SO_3 , [2, 4, 55, 56]. The set of all rotations of a sphere is a useful example of a Lie group. They are a continuous infinity of rotations of an ordinary sphere or 2-sphere, S^2 , which is embedded in SO_3 . The rotations of S^2 form a 3-sphere modular plus or minus 1, called $S^3 / \{ \pm 1 \}$ which is embedded in SO_3 . This group is the set of all special orthogonal 3×3 matrices. The finite subgroups of SO_3 are the symmetry groups of the various polyhedra which are inscribed on the sphere S^2 upon which SO_3 acts. These regular polyhedral groups are the symmetry groups for the five Platonic solids. The octahedron and icosahedron are inscribed in S^2 , the symmetry group of 24 elements for the octahedral group O and the 60 element icosahedral group I . The polyhedral groups T , O and I describe the symmetries of the five Platonic solids.

The octahedron and the cube have the same symmetry group and are dual to each other under the S_4 group. The icosahedron and the dodecahedron are dual to each other under the A_5 group and the 12-element group T is the tetrahedral group of which the symmetries are inscribed in S^2 and is the A_4 group. The 24 element octahedral group is denoted as O and is the set of all symmetries inscribed in S^2 , which is also the symmetry group of the cube since the six faces of the cube correspond to the six vertices of the octahedron and eight faces of the octahedron correspond to the eight vertices of the cube. The relationship of the finite and infinitesimal groups is key to understanding the symmetry relation of particles, matter and force fields or gauge fields and the structural topology of space, i.e. real, complex and abstract spaces. We now relate the toroidal topology and the cuboctahedron geometry to current particle physics.

The 24 element octahedral group is given as $C[\bar{0}] = U_2 \times \tilde{U}_2 \times U_4$ which is mapable to the conformed supergravity group $SU(2,2/1)$. We can write this as $C[0] = U_1 \times U_1 \times SU_2 \times SU_3 \times SU_3$. The U_1 can act as the photon (electromagnetic) gauge invariance group and relates to the rotation group SO_3 . The other U_1 scalar is the base for space and time as the compact gauge group of the spin two graviton. The SU_2 group can be associated with weak interactions and $U(1) \times SU_2$ is the group representation of the electroweak force. The SU_3 groups represent the strong color quark – gluon force or gauge field [55]. See the next section in which the strong and gravitational forces are related to each other.

Thus we have a topological picture that relates to the unification of the four force fields in the Grand Unification Theory, or GUT and supersymmetry models. More exactly, the maximal compact space embedded in $C[OS_4]$ or $U(2, 2/1)$ yields the 24 element conformal supergravity group. The icosahedron or Klein group yields the set of permutations for S_4 permutation group associated with $C[0]$. Also in the Georgi and Glashar [57] scheme we can generate SU_5 as a 24 element group related to S^4 embedded in $SU_5 = SU_2 \times SU_3$. The key to this approach is the relationship of the finite groups $C(0)$ and the Lie group such as the SU_n groups. This picture is put forward in detail by S.P. Sirag [55, 58] in his significant advancement of fundamental particle physics.

The eight (8) fundamental spinor states can be expressed in terms of the Riemann sphere S^2 which defines the relationship of spinors to space-time. The 8 spinor states correspond to the 8 vertices of a cube. For 8 antistates, Sirag can generate all 16 states of the Fermion family for a cube and its mirror image cube and then he utilizes the symmetric four group S_4 which is isomorphic to O , the octahedral group.

As before stated, the cube and octahedron are dual to each other under the symmetry operations of the S^4 group. Also, the tetrahedron has the alternate A_4 group, and the icosahedron and dodecahedron are dual under the A_5 group. The $C[0]$ group or actually the $SU(2, 2/1)$ is the now compact representation of the Yang-Mill Bosons and $C[\bar{0}]$ represents the matter fields of the Fermions. The Weyl group is $SU(2,2)$ which is related to $SU(2, 2/1)$, the Penrose twister [59, 60], which represents a vortical rotational complex dimensional space, mapable to the Kaluza-Klein model which relates the electromagnetic metric to the gravitational metric as a five space [61, 62]. The Penrose twistor is a spin space and is like a double torus without a “waste.” The U_2 group represents the four real spacetime and \tilde{U}_2 the four imaginary spacetime forming a complex eight space [63, 64]. Twistor algebra of this complex eight space is mapable 1 to 1 with the spinor calculus of the Kaluza-Klein geometry, thus the electromagnetism is related to the gravitational spacetime metric [63]. The S_4 and \overline{S}_4 groups are 24 element groups, as S_4 can be associated with $C[0]$ and \overline{S}_4 with $C[\bar{0}]$. The S_4 group is associated with the 24 dimensions of the GUT theory. The conjugate group of \overline{S}_4 is associated with $U_2 \times \tilde{U}_2 \times U_4$ or for U_4 , which are four copies of U_1 , that can be written as $U_1 \times U_1 \times U_1 \times U_1$ where $U_1 \times U_1$ represents a torus, hence U_4 represents a double or dual torus. We have demonstrated that the cover group of the cuboctahedron generates the torus $U_1 \times U_1$ and we demonstrate that the cover group generates the dual torus $U_1 \times U_1$ cross $U_1 \times U_1$ in the Haremeinian topology.

The hourglass topology is directly formed from the topology of the dual sphere. The relationship of the cuboctahedral groups and the dual torus is a fundamental tenant of the Haremein geometric topology and, as seen here, seems to be fundamental for unification [2, 14].

REFERENCES

1. Laura Ferrarese, Black hole Demographics, http://arxiv.org/PS_cache/astro-h/pdf/0203/0203047v1.pdf, arXiv:astro-ph/0203047v1 4 Mar 2002.
2. N. Hamein and E.A. Rauscher, "The origin of spin: a consideration of torque and Coriolis forces in Einstein's field equations and grand unification theory," in *Beyond the Standard Model: Searching for Unity in Physics*, Eds. R.L. Amoroso. B. Lehnert & J-P Vigier, Oakland: The Noetic Press, July (2005).
3. R.W. Lindquist and J.A. Wheeler, "Dynamics of a Lattice Universe by the Schwarzschild-Cell Method", *Rev. of Mod. Phys.*, 29, Num. 432, (1957).
4. Hamein, N. and Rauscher, E.A., "Collective coherent oscillation plasma modes in surrounding media of black holes and vacuum structure - quantum processes with considerations of spacetime torque and Coreolis Forces," in *Beyond the Standard Model: Searching for Unity in Physics*, Eds. R.L. Amoroso. B. Lehnert & J-P Vigier, Oakland: The Noetic Press July (2005).
5. N. Hamein, "Scaling Law for Organized Matter in the Universe," *Bull. Am. Phys. Soc.* AB006, Ft. Worth, Oct. 5 (2001).
6. N. Hamein, "Fundamental Dynamics of Black Hole Physics," *Bull. Am. Phys. Soc.* Y6010, Albuquerque, Apr. 23 (2002).
7. E.A. Rauscher, "Electron Interactions in Quantum Plasma Physics," *J. Plasma Phys.* 2, 517 (1968).
8. NASA, Press release no. STSci-PR 94-22 and no. STSci-PR96-1996.
9. Battaner, "The Fractal Octahedron Network of the Large Scale Structure," *Astrophysics abstract*, astro-ph/9801276, Jan. 28, 1998, <http://xxx.lanl.gov/abs/astro-ph/980126>.
10. Battaner and E. Florido, "The egg-carton Universe," *Astrophysics abstract*, Astro-ph/9802009, Feb. 2, 1998, <http://xxx.lanl.gov/abs/astro-ph/9802009>
11. K. Schwarzschild, Sitzber, Deut. Akad. Wiss. Berlin, KL Math Phys. Tech. 189-196 (1916).
12. J.A. Wheeler *Geometrodynamics*, Academic Press, 1962 and private communication.
13. E.A. Rauscher, *A Unifying Theory of Fundamental Processes*, UCB-LBNL, UCRL 20808, Contract W-7405-48, June 1971.
14. N. Hamein, "A Balance Equation at the Event Horizon" (in progress).
15. R. Barkana and A. Loeb, *Phys. Rev.* 349, 125 (2001)
16. K. Thorne, *Black Holes and Time Warps*, Norton, New York, 1994.
17. E.A. Rauscher, "Closed Cosmological Solutions to Einstien's Field Equations," *Let. Nuovo Cimento* 3, 661 (1972).
18. E.A. Rauscher, "Speculations on a Schwarzschild Universe," UCB/LBNL, LBL-4353, (1975) and *Cosmogenesis and Quantum Gravity*, pp. 43-72, in *Beyond the Standard Model: Searching for Unity in Physics*, Eds. R.L. Amoroso. B. Lehnert & J-P Vigier, Oakland: The Noetic Press, July (2005).
19. E. Abdalla, et al., "Information transport by sine-Gordon solitons in microtubules," <http://arxiv.org/abs/physics/0103042v1>, physics.bio-ph., 15 Mar. 2001.
20. Mario Livio, "Searching for the Golden Ratio," *Astronomy*, Apr. (2003)., pp 52-57.
21. Wikipedia, Penrose tiling, http://en.wikipedia.org/wiki/Penrose_tiles, 2008
22. P. C. W. Davies, "Thermodynamic phase transitions of Kerr-Newman black holes in de Sitter space," *Class. Quantum Grav.* 6, 1909-1914, 1989.
23. A. G. Riess *et al.*, *Astron. J.* 116, 1009 (1998).
24. Choppin, Gregory R., Liljenzin, Jan-Olov, Rydberg, Jan, "Radiochemistry and Nuclear Chemistry," Butterworth-Heinemann, (2001), p. 288.
25. S. K. Lamoreaux, *Phys. Rev.* 78, 5 (1997).
26. U. Mohideen and A. Roy, *Phys. Rev.* 81, 4549 (1998).
27. B. W. Harris, F. Chen, and U. Mohideen, *Phys. Rev.* A62, 052109 (2000).
28. H. B. Chan, V. A. Aksyuk, R. N. Kelman, D. J. Bishop and F. Capasso, *Science* 291, 1941 (2001).
29. G. Bressi, G. Carugno, R. Onofrio and G. Ruoso, "Measurement of the Casimir Force between Parallel Metallic Surfaces," *Phys. Rev. Lett.* 88, 041804-1 (2002).
30. P. M. Garnavich *et al.*, *Astrophys. J.* 509, 74 (1998).
31. S. Perlmutter *et al.*, *Astrophys. J.* 517, 565 (1999).
32. C.W. Misner, K.S. Thorne, and J.A. Wheeler, *Gravitation*, Freedman and Co., (1973), p.1196.
33. *Ibid*, p.1201.
34. NASA press release, "New Energy Source 'Wrings' Power from Black Hole Spin," Oct. 22, (2001).

35. J. Wilms, et al., "XMM-EPIC observation of MCG-6-30-15: Direct evidence for the extraction of energy from a spinning black hole?," arXiv:astro-ph/0110520v1 23 Oct2001, Mon. Not. R. Astron. Soc. 000, 1-6 (2001), February 2008
36. S. W. Hawking, "Virtual Black Holes," arxiv:hep-th/9510029v1 6 oct. (1995).
37. M. Tegmark, A. de Oliveira-Costa A and A J. S. Hamilton , "A high resolution foreground cleaned CMB map from WMAP," arXiv:astro-ph/0302496v4 26 Jul 2003, Submitted to Phys. Rev. D March 4 2003.
38. L. Wang, *et al*, "The Axially Symmetric Ejecta of Supernova 1987A," arXiv:astro-ph/0205337 v1 20 May, (2002) Lifan Wang, *et al*," Spectropolarimetry of the Type Ic SN 2002ap in M74: More Evidence for Asymmetric Core Collapse," arXiv:astro-ph/0206386 v2 21 Jun, (2002).
39. R. S. Nemmen, et al., "Models for jet power in elliptical galaxies: A case for rapidly spinning black holes," Mon. Not. R. Astron. Soc. 000, 1-12 (2006)
40. J. Hsu, "Black Holes Spin Near Speed of Light," Space.com, 15 January 2008
41. J. Jalocha, et al., "Is dark matter present in NGC 4736? An iterative spectral method for finding mass distribution in spiral galaxies," arXiv:astro-ph/0611113v3, 30 Jan 2008.
42. S. Battersby, "Galaxy without dark matter puzzles astronomers," NewScientist.com, <http://space.newscientist.com/article/dn13280-galaxy-without-dark-matter-puzzles-astronomers.html>, February 2008.
43. G. J. Fishman, et al., "Discovery of Intense Gamma-Ray Flashes of Atmospheric Origin," *Science* 27 Vol. 264 no. 5163, pp. 1313 - 131, May 1994.
44. Stanford University Webiste, What Comes Out of the Top of a Thunderstorm - Gamma Rays from Severe Weather <http://www-star.stanford.edu/~vlf/optical/press/fishman99nasa> May 26, 1999.
45. S B. Mende, D. D. Sentman and E. M. Wescott, *Lightning between Earth and Space*, <http://www-star.stanford.edu/~vlf/optical/press/mende97sciam/>, 1997.
46. A. N. Dmitriev, V. L. Dyatlov, and V. I. Merculov, "Electrogravodynamic Concept of Tornadoes," <http://www.tmgnow.com/repository/planetary/tornado.html>
47. E. H. Lewis, "Tornadoes and Ball Lightnings as Plasmoids," <http://www.intenex.net/~elewis/lewispaper/lewis2006tornadoblpaper.doc>, Sciencejunk.org, 2008.
48. P. Charbonneau, et al., "The Rotation of The Solar Core Inferred by Genetic Forward Modeling," *The Astrophysical Journal*, 496:1015-1030, 1998 April 1, 1998.
49. J-P., Zahn Figure 2., Observatoire de Paris, LUTH, www.obspm.fr/actual/nouvelle/jul02/neu-sol.en.shtml 2008.
50. H. J. Lugt, *Vortex Flow in Nature and Technology*, Krieger Publishing Company, Malabar, Florida, 1995.
51. S. Yoshiaki, and V. Rubin, "Rotation Curves of Spiral Galaxies," *Annu. Rev. Astron. Astrophys.* 39:137-74, 2001.
52. Y. Sofue, et. al., "Central Rotation Curves of Spiral Galaxies," <http://www.ioa.s.u-tokyo.ac.jp/~sofue/RC99/paper.htm>, *Astrophysical Journal* Vol. 523, pp136-146, 1999.
53. L. Ferrarese, "Beyond The Bulge: A Fundamental Relation Between Supermassive Black Holes and Dark Matter Halos," *The Astrophysical Journal*, arXiv:astro-ph/0203469 v2 1 Jul 2002.
54. NASA press release, "The Sun's Dark Secret: How Sunspots Pull Themselves Together," Nov. 6 (2001) *Science @ NASA*, "What Lies Beneath a Sunspot: Awesome plasma hurricanes were one of the surprises revealed when scientists recently peered beneath the stormy surface of our star," Nov. 7 (2001).
55. S.P. Sirag, *International Journal of Theoret. Phys.* **22**, 1067 (1983).
56. S.P. Sirag, *Bull. Am. Phys. Soc.* **34**, 1 (1989).
57. H. Georgi and S.L. Glashow *Phys. Rev. Lett.* **32**, 438 (1974).
58. S.P. Sirag, *Bull. Am. Phys. Soc.* **27**, 31 (1982).
59. R. Geroch, A. Held and R. Penrose, *J. Math. Phys.* **14**, 874 (1973).
60. R. Penrose, "The Geometry of the Universe," *Mathematics Today*, ed. L.A. Steen, Springer-Verlag, 1978.
61. Th. Kaluza, *Sitz. Berlin Press, Acad. Wiss.* 199 (1921).
62. O. Klein, *Z. Phys.* **37**, 895 (1926).
63. C. Ramon and E.A. Rauscher, "Superluminal Transformations in Complex Minkowski Spaces," *Found. of Phys.* **10**, 661 (1980).
64. E.A. Rauscher, *Bull. Am. Phys. Soc.* **23**, 84 (1978).